Dna Research, 2017, 24(2), 103–115
doi: 10.1093/dnares/dsw060
Advance Access Publication Date: 29 January 2017
Full Paper

OXFORD

Full Paper

Somatic transposition and meiotically driven elimination of an active helitron family in *Pleurotus ostreatus*

Alessandra Borgognone, Raúl Castanera, Elaia Muguerza, Antonio G. Pisabarro, and Lucía Ramírez*

Genetics and Microbiology Research Group, Department of Agrarian Production, Public University of Navarre, Pamplona, Navarre, Spain

*To whom correspondence should be addressed. Tel. +34 948169130. Fax. +34 948169732. Email: lramirez@unavarra.es

Edited by Prof. Takashi Ito

Received 21 September 2016; Editorial decision 12 December 2016; Accepted 14 December 2016

Abstract

Helitrons constitute a superfamily of DNA transposons that were discovered *in silico* and are widespread in most eukaryotic genomes. They are postulated to mobilize through a "rolling-circle" mechanism, but the experimental evidence of their transposition has been described only recently. Here, we present the inheritance patterns of HELPO1 and HELPO2 helitron families in meiotically derived progeny of the basidiomycete *Pleurotus ostreatus*. We found distorted segregation patterns of HELPO2 helitrons that led to a strong under-representation of these elements in the progeny. Further investigation of HELPO2 flanking sites showed that gene conversion may contribute to the elimination of such repetitive elements in meiosis, favouring the presence of HELPO2 vacant loci. In addition, the analysis of HELPO2 content in a reconstructed pedigree of subclones maintained under different culture conditions revealed an event of helitron somatic transposition. Additional analyses of genome and transcriptome data indicated that *P. ostreatus* carries active RNAi machinery that could be involved in the control of transposable element proliferation. Our results provide the first evidence of helitron mobilization in the fungal kingdom and highlight the interaction between genome defence mechanisms and invasive DNA.

Key words: helitrons, segregation distortion, gene conversion, transposable elements, basidiomycete

1. Introduction

Transposable elements (TEs) constitute an important fraction of the eukaryotic and prokaryotic genomes. These DNA fragments are able to mobilize in the host genome, contributing to chromosomal rearrangements and transcriptional modulation.[1] On the basis of their transposition mechanisms, TEs can be grouped into two classes: Class I TEs transpose by a copy-and-paste mechanism *via* RNA intermediates, and Class II TEs proliferate via DNA intermediates using cut-and-paste transposition or rolling-circle replication.[2,3] The vast majority of TEs produce target site duplications (TSDs) at their insertion sites, with some exceptions as Helitrons, a subclass of DNA transposons discovered in 2001 by computational analysis in *Arabidopsis thaliana*, *Oryza sativa*, and *Caenorhabditis elegans* genomes.[3] Helitrons are present in a wide range of eukaryotic genomes[3–6] and show several structural and enzymatic features that differentiate them from the rest of the TEs. They do not display terminal inverted repeats as other DNA transposons do, do not generate TSDs at the insertion site, and carry conserved 5'-TC and

© The Author 2017. Published by Oxford University Press on behalf of Kazusa DNA Research Institute.
This is an Open Access article distributed under the terms of the Creative Commons Attribution Non-Commercial License (http://creativecommons.org/licenses/by-nc/4.0/), which permits non-commercial re-use, distribution, and reproduction in any medium, provided the original work is properly cited. For commercial re-use, please contact journals.permissions@oup.com

Downloaded from https://academic.oup.com/dnaresearch/article-abstract/24/2/103/2962881
by Universidad Pública de Navarra user
on 09 August 2018

CTRR-3' ends and a 16–bp palindromic hairpin located approximately 10–20 nucleotides upstream of the 3' terminus.[3,7] Additionally, putative autonomous helitrons encode a RepHel protein containing a replication initiation (Rep) and a helicase (Hel) domain. The conservation of the Rep catalytic motifs with the replication initiators of plasmids and ssDNA viruses led to the hypothesis that these elements transpose with a rolling-circle mechanism (RC), which is consistent with the absence of TSDs. Nevertheless, a study carried out in maize haplotypes identified helitron somatic excision events based on the presence of footprints in polymorphic helitron loci (occupied *vs* vacant loci occurrence in the genome),[8] suggesting that this TE subclass may show both excision and replication based transposition mechanisms. Similar to other transposons, it has been described that helitrons can promote rearrangements in plant genomes[9,10] and generate intra-specific variability by breaking the genetic co-linearity among haplotypes.[9–11] In addition, during the transposition process, helitrons can capture and disperse gene fragments, producing chimeric transcripts.[9] After their discovery, *in silico* studies have been carried out to characterize the nature of these eukaryotic DNA TEs. Despite several helitron-related finding being described and explained, the mechanism of helitron mobilization remained unclear because, until very recently, there was no experimental evidence for their transposition. Interestingly, a novel study reports the first experimental evidence of helitron insertions in cell culture, providing insights into the transposition and gene capture mechanisms.[12] In addition, the finding of circular DNA intermediates containing head-to-tail junctions of helitron ends strongly supports the originally proposed RC transposition mechanism.[5,12] Previous bioinformatics analyses have reported that helitrons account for 0-3% of the mammalian genome size[5,13] and 1–5% of the genome size in insects.[4,7] In plants, these DNA transposons constitute a variable portion, contributing between 0.01 and 6% among different species.[3,14–16] In fungi, the presence of helitrons has been reported often as part of *in silico* comprehensive TE annotations of several ascomycetes and basidiomycetes sequenced genomes.[7,17–21] In addition, a study in *Aspergillus nidulans* described the capture and duplication of a gene promoter during the generation of a non-autonomous helitron.[18] In *P. ostreatus*, a recent study carried out in our group identified and characterized two helitron families, HELPO1 and HELPO2, which showed differential patterns of expression and distribution. *P. ostreatus* has been widely studied due to its agronomic importance and also due to its ability to selectively degrade lignin.[22,23] The simplicity of its life cycle and its ability to grow and fructify under laboratory conditions make it an interesting model for fungal genetics. The *P. ostreatus* life cycle alternates between monokaryotic and dikaryotic mycelial phases containing haploid and diploid nuclei. Two compatible monokaryons can fuse and generate a dikaryon (the sexually competent form) in which the two parental nuclei remain separated during vegetative growth and fruit body development. The karyogamy (diploid condition) occurs only in the basidia at the end of the life cycle, immediately before the meiotic division that produces four haploid basidiospores. The two nuclei harboured in the *P. ostreatus* dikaryotic strain N001 were isolated by a de-dikaryotization process based on the protoplast obtained by an enzymatic treatment of the mycelium of the dikaryotic strain N001 and the subsequent identification of the monokaryons derived from protoplasts containing either of the two nuclei.[24] This process yielded two compatible protoclones (monokaryons PC15 and PC9) bearing each one of the non-recombined haploid nuclei. The availability of these strains, as well as a meiotic progeny derived from the N001 dikaryotic strain, enabled further genetic studies of *P. ostreatus*. Specifically, the molecular karyotype determined the presence of 11 chromosomes[24] that fit with 11 linkage groups described by our group in the genetic linkage map of *P. ostreatus*.[25,26] These studies supported the subsequent genome sequencing of PC9 and PC15 protoclones. Both genomes showed an overall conserved macrosynteny, but the sequencing and annotation unraveled remarkable genomic differences in regions corresponding to TEs. In a recent study, 80 TE families were identified accounting for 2.5 and 6.2% of PC9 and PC15 genome sizes, respectively. The results of this work showed that the *P. ostreatus* genome is mainly populated by LTR-retrotransposons. Nevertheless, helitrons were the most abundant DNA transposons in the genome, and the HELPO1 family was among the most expressed TE families. *P. ostreatus* helitrons carry most canonical features such as the 3' subterminal hairpin and the RepHel helicase. Nevertheless, in contrast to plants and animal helitrons, their encoded helicase does not carry RPA or zinc fingers domains.[17,27] They represent up to 0.35% of the *P. ostreatus* genome and are frequently displayed in polymorphic loci of PC15 and PC9. In the present study, we used experimental approaches to uncover the differential amplification dynamics of helitrons in *P. ostreatus* subclones maintained on solid culture under high- and low-subculture frequencies. In addition, we analysed the pattern of inheritance of helitron TEs in the offspring of 68 monokaryotic strains meiotically obtained from the dikaryotic strain N001. We provide evidence of somatic HELPO2 transposition in one of the analysed subclones and show that the HELPO2 family is under-represented in the progeny. A detailed analysis of two HELPO2 loci suggests that helitrons could be eliminated during meiosis by gene conversion.

2. Materials and methods

2.1. Origins of the *P. ostreatus* monokaryotic and dikaryotic strains

A total of 74 strains and sub-clones of *P. ostreatus* with different nuclear allelic compositions were used in this study. All of them were derived from N001, a dikaryotic strain used by our group as a model for mushroom breeding, genetics and genomics since 1994.[28] The N001 strain was de-dikaryotized in 1999, and the two corresponding haploid-monokaryotic protoclones were recovered and identified as PC9 and PC15.[24] Both monokaryotic strains have been sequenced by the Joint Genome Institute, and their genome assemblies and annotations are publicly available in the Mycocosm Database.[27,29,30] For each of the three strains, a subclone was deposited in the Spanish Type Culture Collection (CECT) on the dates indicated in Table 1 and maintained under low subculture frequency (N001-03, PC9-99 and PC15-99, two subcultures per year); another subclone was kept under high subculture frequency (approximately 8 subcultures per year) for routine laboratory workup to the present day (N001-14, PC9-14 and PC15-14). In addition, we used a haploid-monokaryotic progeny of 68 monokaryotic strains meiotically derived from N001 in 1994 (68 mK; Table 1). This collection has been stored in our laboratory for 20 years under low subculture frequency.

2.2. Culture conditions and nucleic acid extraction

All of the strains and subclones used in this work were cultured in liquid SMY submerged fermentation (10 g of sucrose, 10 g of malt extract, 4 g of yeast extract, 1 l H_2O [pH 5.6]) in the dark at 24 °C under orbital shaking (130 rpm). The cultures were kept for eight growing days, and the mycelia were collected using vacuum

Downloaded from https://academic.oup.com/dnaresearch/article-abstract/24/2/103/2962881
by Universidad Pública de Navarra user
on 09 August 2018

Table 1. Description of *P. ostreatus* strains and subclones used in this study

Subclone	Strain	Nuclear condition (ploidy)	Subculture regime (frequency)	Use/storage	Culture period
N001-03	N001	Dikaryon (n+n)	High/Low[a]	Culture Collection (CECT20600)	1994–2003/2003–2014
N001–14	N001	Dikaryon (n+n)	High (8/year)	Laboratory work	1994–2014
PC9-99	PC9	Monokaryon (n)	Low (2/year)	Culture Collection (CECT20311)	1999–2014
PC9-14	PC9	Monokaryon (n)	High (8/year)	Laboratory work	1999–2014
PC15-99	PC15	Monokaryon (n)	Low (2/year)	Culture Collection (CECT20312)	1999–2014
PC15-14	PC15	Monokaryon (n)	High (8/year)	Laboratory work	1999–2014
68 mK[b]	N001 – single spore isolates	Monokaryon (n)	Low (2/year)	Culture Collection (Laboratory)	1994–2014

[a]This subclone was maintained under high subculture frequency from 1994 to 2003. Then, it was deposited in the CECT and maintained under low subculture frequency on solid medium until 2014.

[b]Collection of 68 mK strains.

filtration, ground in a sterile mortar in the presence of liquid nitrogen and stored at −80°C. Genomic DNA extractions were carried out using an E.Z.N.A. Fungal DNA Mini Kit (Omega Bio-Tek, Norcross, GA), following the manufacturer's instructions. After additional incubation with 4 µl of RNAse A (10 mg/ml) for 30 minutes at 37°C, the DNA solutions were treated twice with phenol-chloroform (3:1), and the pellet was resuspended in 40 µl of nuclease-free water. DNA concentrations were determined using a Qubit 2.0 fluorometer (Life Technology, Carlsbad, CA). The evaluation of total DNA purity was based on the Nanodrop™ 2000 A_{260}/A_{280} ratio (Thermo Scientific, Wilmington, DE). DNA preparations served as a template for both real-time quantitative polymerase chain reaction (qPCR) and conventional PCR approaches.

2.3. Design and validation of primer sequences

Primers were designed based on the *P. ostreatus* reference genome sequences PC15 v2.0 and PC9 v1.0 (http://genome.jgi.doe.gov/PleosPC15_2/PleosPC15_2.home.html), using Primer3 software.[31] Specificity of primer pairs was verified *in silico* by two approaches: (i) BLASTN searches[32] against *P. ostreatus* genomes using primer sequences as a query and (ii) manual verification of perfect matches between oligonucleotides and binding sites in PC15_PC9 alignments of the target loci. The validated primers were used to perform experimental analyses based on qPCR and conventional PCR.

2.4. Real-time quantitative PCR analysis

The helitron content was estimated by qPCR using a relative quantification approach.[33] Reactions were carried out in a CFX96 thermal cycler (Bio-Rad Laboratories, S.A.). Amplification products were monitored at each cycle of PCR using SYBR green fluorescent dye. Each amplification mixture (20 µl) contained 1X IQ SYBR green Supermix (10 µl), 6 µM forward and reverse primers and 0.5 ng of genomic DNA in nuclease-free water. Primers were designed targeting family-specific regions to selectively amplify the HELPO1 and HELPO2 elements. The list of primers designed for the amplification of helitrons and reference single-copy genes is shown in Supplementary Table S1. Reactions were run according to the following cycling conditions: DNA templates were denatured at 95°C for 5 min, followed by 40 cycles of amplification (95°C for 15 s, 60°C for 30 s, and 95°C for 1 min). The final melting curve was set by increasing 0.5°C every 5 sec from 65 to 95°C. Each assay was performed in triplicate in 96-well plates, and a non-template control for each primer pair was included. Relative fluorescence units and threshold cycle values were processed using Bio-Rad CFX Manager Software, and the results were exported to Microsoft Excel for further analysis. The helitron copy number was estimated as a relative value in relation to the average signal of two single-copy reference genes, according to Equation (1):

$$\mathrm{RCN} = 2^{-\,(\mathrm{Ct}hel\,-\,\mathrm{Ct}ref)} \quad (1)$$

where RCN stands for relative copy number, Ct_{hel} is the threshold cycle value of the target region (helitron) and Ct_{ref} is the average threshold cycle value of *sar1* and *lacc3* single-copy reference genes.

2.5. Conventional PCR reactions

Several PCR protocols were designed according to the amplicon size and were run on a thermal cycler PCT-200 (MJ Research, MN). Biotaq DNA Polymerase (Bioline, Luckenwalde, Germany) was used to amplify products lower than 3.5 kb. Each PCR mix was performed in a final volume of 25 µl containing 1 unit of Biotaq polymerase, 50 mM $MgCl_2$, dNTP mix at 100 mM, and forward and reverse primers at 6 µM. Template DNA was firstly denatured at 95°C for 5 min followed by 30 cycles of amplification (95°C for 40 s, 58°C for 60 s, 72°C for 1–3 min, depending on the expected product size) and a final extension cycle at 72°C for 10 min. RANGER DNA Polymerase (Bioline, Luckenwalde, Germany) was used to amplify products longer than 3.5 kb. PCR reactions were prepared following the manufacturer's recommendations in a final volume of 50 µl containing 4 units of RANGER DNA polymerase, 20 µM of specific primers and 20 ng of total DNA template suspended in nuclease-free water. PCR conditions comprised initial denaturation at 95°C for 3 min followed by 30 cycles of 98°C for 10 s, 57°C for 60 s and 68°C for 5–10 min (depending on the expected product size), with a final extension at 68°C for 10 min. For both protocols, negative controls were included using nuclease-free water instead of DNA template. Amplicons were resolved by electrophoresis on 0.8% w/v TAE agarose gels (1X Tris-acetate-EDTA), stained with 1:20,000 Red Safe™ (iNtRON Biotechnology) and visualized under UV Illumination. PCR products were isolated from the agarose gels, purified with an E.Z.N.A Gel Extraction Kit (Omega Bio-Tek, Norcross, GA) and sequenced using Sanger technology (Sistemas Genómicos S.L.,Valencia, Spain and Genewiz Incorporated, South Plainfield, NJ). Primer pairs used for the conventional PCR approach are listed in Supplementary Tables S2–S5.

Downloaded from https://academic.oup.com/dnaresearch/article-abstract/24/2/103/2962881
by Universidad Pública de Navarra user
on 09 August 2018

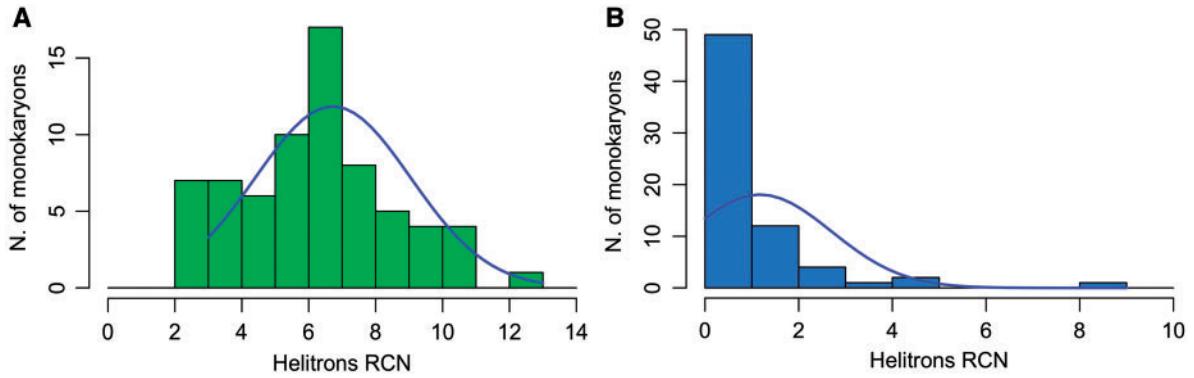

Figure 1. Distribution of HELPO1 (A) and HELPO2 (B) relative copy number in the 68-mK meiotic population. Relative copy numbers are presented as histograms with density lines.

2.6. Detection of RNAi pathway genes in *P. ostreatus*

Key genes involved in Quelling and Meiotic Silencing of Unpaired DNA (MSUD) pathways described in *Neurospora crassa* were used as a query for BLASTP searches (cutoff e value $= e^{-5}$) against *P. ostreatus* PC15 v2.0 and PC9 v1.0 annotations. GenBank accessions of *N. crassa* proteins were the following: *qde-1*: EAA29811.1, *qde-2*: ESA42123.1, *qde-3*: AAF31695.1, *sad-1*: AAK31733.1, *sms-2*: EAA29350, *dcl-1:* EAA32662.1, *dcl-2*: EAA34302.3, and *qip*: XP_011393741.1. Conserved domains of *P. ostreatus* proteins with significant hits were identified using HMMER3 software[34] with PFAM-A target database,[35] as well as NCBI Conserved Domain Database.[36] In parallel, proteins were clustered using all by all BLASTP (cutoff e value $= e^{-10}$) followed by mcl[37] (inflation value $=2$). Clusters of proteins carrying the same conserved domains as the query proteins were retained. Orthology between PC15 and PC9 proteins was inferred by reciprocal best blast hit.

3. Results and discussion

3.1. HELPO1 and HELPO2 families show different inheritance patterns in the N001 meiotic progeny

To analyse the inheritance patterns of the two helitron families present in *P. ostreatus*, we studied helitron segregation in a progeny of 68 monokaryons meiotically derived from the N001 strain (population 68 mK) by means of qPCR. The relative copy number of HELPO1 elements showed a normal distribution in the progeny (Shapiro-Wilks test, $W = 0.978$, $P = 0.271$), with monokaryons displaying RCN values ranging from 2 to 13 and a population peak showing 6–7 RCNs (Fig. 1A). Surprisingly, results corresponding to the HELPO2 family showed a trend that did not fit with a normal distribution ($W = 0.727$, $P = 5.135\ e^{-10}$, Fig. 1B). In this case, although RCNs ranged from 0 to 9, up to 49 monokaryons exhibited only 0 or 1 helitrons, uncovering a strong bias towards the lack of HELPO2 elements in the N001 progeny. Previous studies carried out by our group indicated that the HELPO2 family amplified very recently in the protoclone PC15, whereas it is absent in the compatible strain PC9.[17] The distorted segregation of HELPO2 elements might be the consequence of a specific genome defence mechanism against the invasion of repetitive DNA. In this sense, the HELPO2 family shows elements with high similarity among them and low transcription levels,[17,27] indicating that it might be targeted by transposon-silencing mechanisms. In contrast, HELPO1 elements are more divergent and showed very high transcription levels.[17,27] This fact suggests that this family is not targeted by genome defense mechanisms. A possible explanation for the unique profile of HELPO2 might be the very recent amplification of RepHel-coding elements in this family, evidenced by the presence of five identical full-length copies. These elements could be detected as foreign, invasive DNA and targeted by the genome defense machinery. To understand the striking differences found in the inheritance patterns of HELPO1 and HELPO2 families in the meiotic progeny, we reconstructed the pedigree of the monokaryotic collection along with their parental strains N001, PC15 and PC9 (Fig. 2), which have been used as a genetic model of study since 1994.

3.2. HELPO2 dynamics diverge in subclones maintained under different subculture conditions

The abundance of HELPO1 and HELPO2 elements was estimated in several subclones of the monokaryons and dikaryon parental strains. These subclones have been stored under different subculture frequencies for up to 20 years, as shown in Table 1 and Fig. 2. Using the previously described qPCR approach, we observed that HELPO1 RCNs were largely conserved and consistently identical among the subclones maintained under a low subculture frequency (PC9-99, PC15-99, N001-03) and the corresponding subclones maintained in the laboratory at a high subculture frequency (PC9–14, PC15–14 and N001-14; $P < 0.05$, two-tailed Student's *t*-test, Fig. 3A). Furthermore, the RCNs observed in N001 dikaryon subclones fit with the sum of PC9 and PC15 RCNs, as expected for an additive model (N001 is a dikaryotic strain that carries the PC15 and PC9 nuclei). In contrast, the estimation of HELPO2 abundance in the monokaryotic and dikaryotic subclones revealed an unexpected scenario. Significant differences were found in HELPO2 content within PC15 and N001 subclone pairs (Fig. 3B). More specifically, PC15-99 showed a RCN value higher than PC15-14 (23 vs 15, respectively), whereas N001-14 showed a striking 5-fold increment in comparison to N001-03 (11 vs 2 RCNs). In the case of PC9, both subclones lacked HELPO2 elements. Previous bioinformatics analysis reported a widespread distribution of HELPO2 copies in the chromosomes of PC15, whereas no intact HELPO2 helitrons were detected in the genome of the PC9 strain.[17] In this sense, qPCR results confirmed the lack of HELPO2 elements in both PC9-99 and PC9-14 strains. Nevertheless, the differential HELPO2 content in the PC15 and N001 subclones suggested that these elements have been mobilized in the mycelia (somatic transposition) and accumulated in the genome as a result of a continuous subculture. The fact that the addition

Downloaded from https://academic.oup.com/dnaresearch/article-abstract/24/2/103/2962881
by Universidad Pública de Navarra user
on 09 August 2018

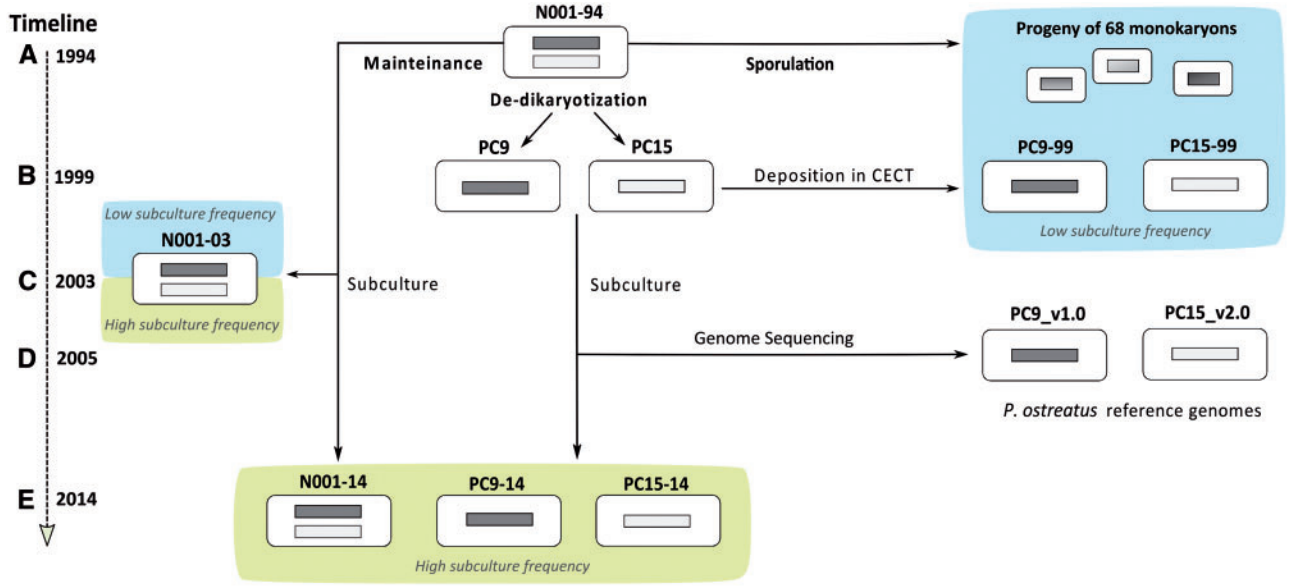

Figure 2. Pedigree and related time-scale events of *P. ostreatus* strains and subclones used in this study. (a) (1994) The N001-94 strain was sporulated leading to the monokaryotic population 68 mK. (b) (1999) PC9 and PC15 protoclones were obtained from N001 by de-dikaryotization and deposited in CECT (PC9-99 and PC15-99). (c) (2003) N001 was deposited in CECT (N001-03). (d) (2005) PC9 and PC15 protoclones were sequenced at JGI. (e) (2014) N001-03, PC9-99 and PC15-99 were retrieved from CECT and used in this study, along with N001-14, PC9-14 and PC15-14 subclones used for laboratory routine work up to 2014.

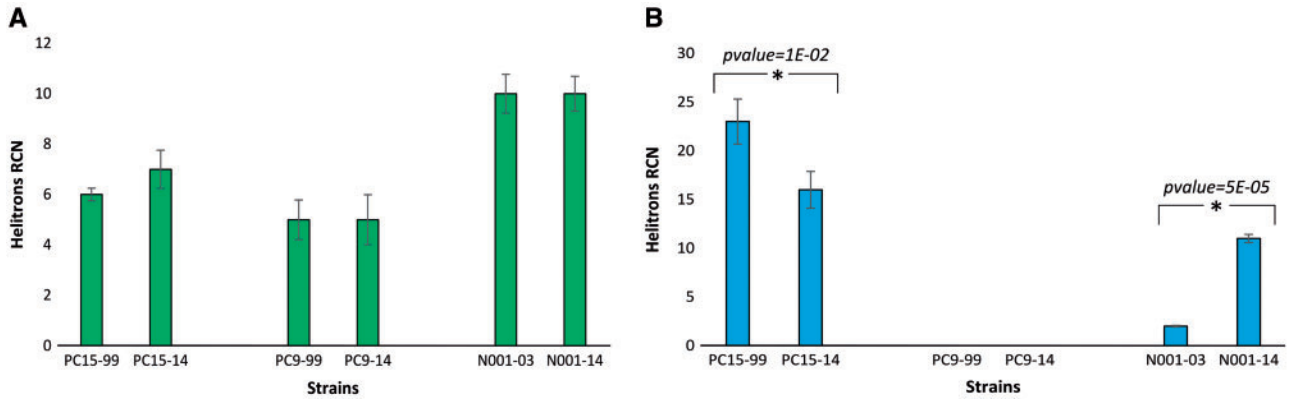

Figure 3. HELPO1 (A) and HELPO2 (B) relative copy number in parental subclones maintained under different subculture frequencies. Relative copy number of elements belonging to HELPO1 and HELPO2 families examined in the dikaryotic (N001) and monokaryotic (PC15 and PC9) parental strains. Data are reported as the mean ± SD.

of PC15 and PC9 HELPO2 RCNs surpasses that of any of the N001 subclones reinforces the hypothesis of an amplification burst in both PC15 subclones. Previous studies have described an amplification burst of DNA transposons (*IS30* and *IS5*) in bacterial subclones maintained for decades in stab culture, giving rise to genetic and phenotypic diversity.[38] In addition, it is known that environmental stresses increase transposition rates.[39,40] In this sense, the de-dikaryotization process underwent by the strain N001 in 1999 might have played a critical role in helitron increases, as protoplast isolation requires an enzymatic digestion protocol that could have triggered a stressful scenario leading to HELPO2 elements activation. We hypothesize that high subculturing rates may increase the chance of helitron transposition and accumulation. The 5-fold increment of the HELPO2 element content in N001–14 vs N001-03 supports this hypothesis, but does not explain the results observed in PC15-99 and PC9-14. In the latter case, the subclone maintained under low-subculturing frequency (PC15-99) shared a higher HELPO2 RCNs than its counterpart maintained under higher subculturing rates. This finding suggest that TE insertions without strong deleterious effects have a random chance of being passed to successive generations by clonal subculturing, thus bringing to the equation a randomness parameter. On the contrary, HELPO1 family elements did not show any sign of amplification. This finding, along with the uniform patterns of its inheritance found in the N001 mk68 meiotic progeny suggested that transposition of HELPO1 elements is infrequent in the *P. ostreatus* genome.

3.3. Molecular analysis of HELPO2 polymorphisms uncovers HELPO2 transposition events

The results obtained by the qPCR approach strongly suggest that HELPO2 is an active family, and the RCN increments observed in

Downloaded from https://academic.oup.com/dnaresearch/article-abstract/24/2/103/2962881
by Universidad Pública de Navarra user
on 09 August 2018

PC15 and N001 suggest that new elements of this family could be populating unknown loci. Previous bioinformatics analyses identified seven HELPO2 copies encoding RepHel helicases, distributed in 5 of 11 nuclear chromosomes of PC15 (Table 2). This genome-wide helitron annotation was carried out with *P. ostreatus* PC9 v1.0 and PC15 v2.0 genome assemblies[17] produced by the JGI in 2005. Using conventional PCR, we re-analysed the parental subclone pairs to track the presence or absence of such HELPO2 loci. The objective of this approach was to confirm the bioinformatics predictions and to identify putative helitron polymorphisms between and within subclone pairs that could be the result of helitron mobilizations. A PCR strategy was designed to differentiate the two possible allelic states corresponding to the presence or absence of a helitron element in a given locus. We designed two primer pairs per locus flanking the left and right helitron ends. In each pair, one primer was designed inside the element, and the other was designed outside the helitron boundary, as shown in Fig. 4A and B. This strategy (outer/inner) allowed us to identify loci carrying HELPO2 insertions ("occupied loci") with positive PCR products, but no amplification should occur in loci with no HELPO2 insertion ("vacant loci"). As expected, none of the PC9 subclones showed amplification in any of the HELPO2 loci (Table 3, Supplementary Fig. S1). Interestingly, a striking difference was observed between PC15-99 and PC15-14 subclones: although the first one displayed HELPO2 insertions in the seven loci described in Table 2, the latter showed no amplification in *Helpo2_I* and in *Helpo2_VIII_c*. Intriguingly, both N001 subclones (N001-03 and N001-14) showed an identical profile to PC15-14 (Table 3, Supplementary Figs. S1A and G). This result leads us to hypothesize that *Helpo2_I* and *Helpo2_VIII_c* helitrons were transposed and inserted exclusively in PC15-99 subclone, after the de-dikaryotization of N001 in 1999. The experimental evidence of helitron transposition has been recently demonstrated in vitro using a reconstructed element from the bat genome.[12] Our finding represents the first evidence of a fungal helitron transposition in its host genome under laboratory conditions. PCR products corresponding to *Helpo2_I* and *Helpo2_VIII_c* were purified, sequenced by Sanger technology and aligned to PC15 v2.0 and PC9 v1.0 genome sequences. The results obtained confirmed the helitron presence in the *Helpo2_I* locus, with the alignments spanning both external and internal regions of the HELPO2 (Fig. 5). Regarding *Helpo2_VIII_c*, it is noteworthy that the PCR product of the right flank displayed a size 0.6 kb larger than expected. In this case, sequenced PCR products could be aligned to the internal helitron regions but not to the external ones due to the low quality of the sequence. To discard that this phenomenon as a false-negative, we designed a second strategy to validate vacant sites with a positive PCR product. Using the PC15 sequence as a reference, primers were designed for regions adjacent to HELPO2 boundaries and homologous to the PC9 regions flanking the vacant site (outer/outer, Fig. 4A). The complexity of such regions (often carrying other transposons, especially *Gypsy* LTR-retrotransposons) made it difficult to find homologous regions between PC15 and PC9, yielding long expected PCR fragment sizes for vacant sites, ranging from 2,603 to 8,578 bp (Supplementary Table S3). To overcome this problem, we used a long-range DNA polymerase that allowed us to amplify vacant and occupied sites including PCR product size up to 10–15 kb (i.e. Fig. 4C). The presence of vacant sites was tested in all subclones (Table 4, Supplementary Fig. S2) including the discordant *Helpo2_I* and *Helpo2_VIII_c* loci in the PC15-99 subclone, despite the outer/inner strategy confirming the presence of HELPO2 in both of them. Using this approach, we validated all vacant sites except PC9 *Helpo2_VII*. This particular locus was further analysed with additional primer pairs and could not be amplified in any of the PC9 subclones, probably due to the inefficacy of long-range RANGER polymerase. Remarkably, the amplification and sequencing of *Helpo2_I* and *Helpo2_VIII_c* in PC15-99 revealed products corresponding to vacant sites, even though we had previously validated the presence of HELPO2 helitrons in both loci by the outer-inner strategy. Validation of these two vacant sites was performed by sequencing and subsequent alignment to the PC15 v2.0 reference (Supplementary Fig. S3). These results could suggest that cells with and without HELPO2 elements (HELPO2+/HELPO2-) coexist in hyphae of the PC15-99 subclone, giving rise to a mosaic mycelium. This fact reinforces the hypothesis of a very recent transposition of both elements, which were not entirely fixed or eliminated from the PC15-99 subclone in the successive subculturing performed after their insertion. In addition, these results provide indirect evidence that helitron was mobilized by replicative or semi-replicative transposition, as HELPO2 elements increased in PC15–99 without the excision of any of the other five occupied loci.

3.4. Distorted segregation patterns of HELPO2 in the N001 meiotic-derived progeny

We investigated the segregation patterns of the seven HELPO2 loci in 68 monokaryons using the previously described outer/inner strategy. As N001 is a dikaryon formed by the mating of PC15 and PC9 monokaryons and due to the seven loci being polymorphic (the presence of helitrons in PC15 vs absence of helitrons in PC9), it should be expected that there is a proportion of 1:1 (presence vs absence of helitrons) in the progeny. In contrast, the results revealed that the inheritance of HELPO2 elements was clearly distorted (Fig. 6). First of all, three of the seven loci carrying a HELPO2 in the PC15 strain (*Helpo2_I*, *Helpo2_VII* and *Helpo2_VIII_c*) were completely absent in the progeny. The fact that *Helpo2_I* and *Helpo2_VIII_c* were present in the PC15-99 subclone but absent in the PC15-14, N001-03, N001-14 and the whole N001 progeny (68 mK) reinforces the hypothesis of its unique (and recent) transposition in PC15-99, which according to this result, would have taken place after N001 de-dikaryotization (1999) but before PC15 genome sequencing (2005), as both loci carry HELPO2 elements in the PC15 v2.0 assembly. This observation demonstrated that these loci were vacant in the original PC15 and PC9 strains that mated in the wild to form N001. Following similar reasoning, a HELPO2 element must have been inserted in *Helpo2_VII* in the PC15 nucleus of the N001 dikaryon in the time that elapsed between the isolation of the meiotic progeny (in 1994 all monokaryons carry a vacant locus) and N001 de-dikaryotization (1999, PC15 carries an occupied locus; Fig. 2). Furthermore, PC9 helitron (vacant) alleles were consistently overrepresented in a ratio close to 3:1 in the remaining four loci. These results are in concordance with the biased distribution of HELPO2 elements previously found in the monokaryotic collection by qPCR (Fig. 1B). This scenario suggests the occurrence of a preferential selection of PC9 helitron (vacant) alleles during meiosis, or, in other words, an elimination of helitrons. To rule out the possibility that such a finding was derived from an artificially skewed progeny, we revisited the *P. ostreatus* genetic linkage map. This map was constructed based on the segregation of 214 molecular markers in a population of 80 sibling monokaryons meiotically derived from N001,[26] and 68 of them were used in this study. According to the genetic map, 86% of the markers followed the expected 1:1 ratio. Additionally, the segregation of genetic markers surrounding HELPO2 loci did not show distorted segregation. Taking together,

Downloaded from https://academic.oup.com/dnaresearch/article-abstract/24/2/103/2962881
by Universidad Pública de Navarra user
on 09 August 2018

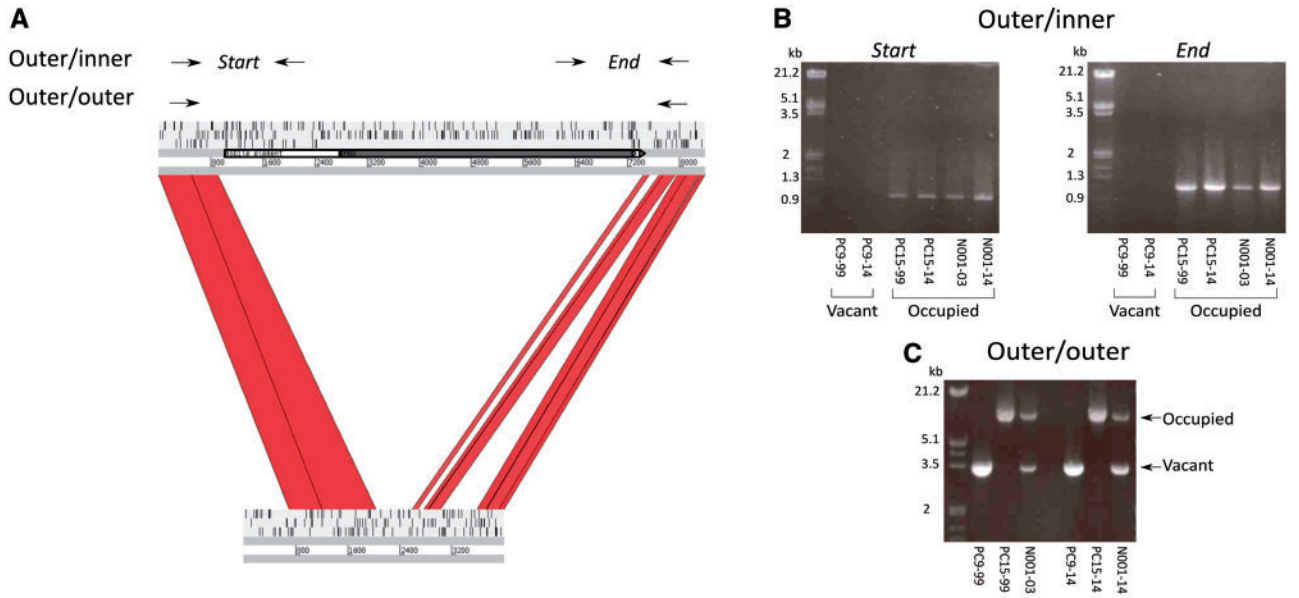

Figure 4. Detection of HELPO2 polymorphisms by the outer/inner and outer/outer strategies. (A) Example of a HELPO2 (*Helpo2_VIII_a*) polymorphic site in PC15 and PC9 haplotypes shown as an ACT (Artemis Comparison Tool) comparison. Blocks indicate conserved regions (>85% similarity). The HELPO2 element is shown as a white arrow with a grey rectangle inside the arrow representing its encoded RepHel helicase. Vertical black lines show stop codons predicted in the three forward reading frames. (B) and (C) represent the amplification profiles of a polymorphic HELPO2 locus in PC9 (vacant), PC15 (occupied) and N001 (vacant + occupied) subclones using the outer/inner and outer/outer strategies.

these data reinforced the fact that the segregation of HELPO2 elements is selectively skewed with respect to the expected Mendelian segregation.

3.5. Somatic transposition of HELPO2 generates mosaicism in *P. ostreatus*

The transposition of an autonomous HELPO2 element to a new chromosomal location in PC15-99 (i.e. *Helpo2_I*, chromosome I, position 619,761-626,150) was validated by two PCR strategies and reinforced by the presence of a vacant locus in the other strains/subclones, including the monokaryotic progeny. We integrated these results in the reconstruction of the pedigree of *P. ostreatus*' strains maintained under different subculture conditions to propose a timescale model that could explain the HELPO2 transposition in PC15-99 and the current HELPO2 profiles obtained in all the strains under study (Fig. 7). After 1999, a somatic transposition of the helitron HELPO2 took place in the nucleus of a cell of a PC15 culture plate and was integrated in the *Helpo2_I* locus by a copy and paste mechanism that could be triggered by the stress of the de-dikaryotization process. As a result, the transposition event originated a new HELPO2 copy in such a cell, which after mitotic replication led to the occurrence of mosaicism in the PC15 mycelia, displaying *Helpo2_I*+ (occupied) and *Helpo2_I*- (vacant) cells. Thus, subsequent subclones derived from the PC15 strain might have been originated from agar plugs located in different sections of the mycelium plate, thus presenting polymorphic loci. We hypothesize that the PC15-14 sample maintained during 20 years under high subculture frequency and used for routine laboratory work could have derived from a section of the PC15 *Helpo2_I*- cells. Alternatively, another likely explanation could be that *Helpo2_I*+ cells were also sampled but lost in the PC15-14 subclone after multiple subculturing replications due to lower fitness in comparison to *Helpo2_I*- or simply by the result of random drift. In contrast, PC15-99 still maintains the phenotype of a genetic mosaic. In this sense, the minimal subculturing frequency of this subclone likely favoured the preservation of both *Helpo2_I*+ and *Helpo2_I*- cells in the same mycelium net. The presence of mosaicism in basidiomycetes has been widely studied in *Armillaria gallica*, where variable numbers of nuclei genotypes have been detected in single fruiting bodies collected for decades.[41] In this sense, it has been described that among-cell-line genetic variation in the haploid mycelium of *A. gallica* may confer plasticity to adapt to changing environmental conditions.[42]

3.6. Allelic gene conversion may contribute to the elimination of HELPO2 helitrons from *P. ostreatus* progeny

As was previously described, the PCR strategies leading to an understanding of the inheritance patterns of the HELPO2 family in the progeny of N001 uncovered an over-transmission of the HELPO2-vacant alleles from the parental PC9. To understand if such phenomena were derived from a preferential inheritance or by helitron excisions during meiosis, we proceeded as follows: *Helpo2_VI* and *Helpo2_VIII_b* loci were chosen on the basis of their clear distortion segregation ratios. All the monokaryons carrying vacant sites according to the lack of amplification by the outer/inner strategy (58 of 68 for *Helpo2_VI* and 55 of 68 for *Helpo2_VIII_b*) were subjected to additional amplification reactions using the primers shown in Fig. 8A and B. The objectives were as follows: (i) to validate the presence of vacant sites with a positive PCR product and (ii) to determine the parental (PC9 or PC15) origin of such vacant sites as well as that of the adjacent regions (i.e. if they were inherited from the parental PC15 or PC9). For this purpose, primers were designed to amplify homologous regions of the parental strains carrying small indels and single nucleotide polymorphisms (SNPs), which allowed us to identify their PC9 or PC15 origin (primer sequences shown in Supplementary Tables S4 and S5). For each locus, the four

Downloaded from https://academic.oup.com/dnaresearch/article-abstract/24/2/103/2962881
by Universidad Pública de Navarra user
on 09 August 2018

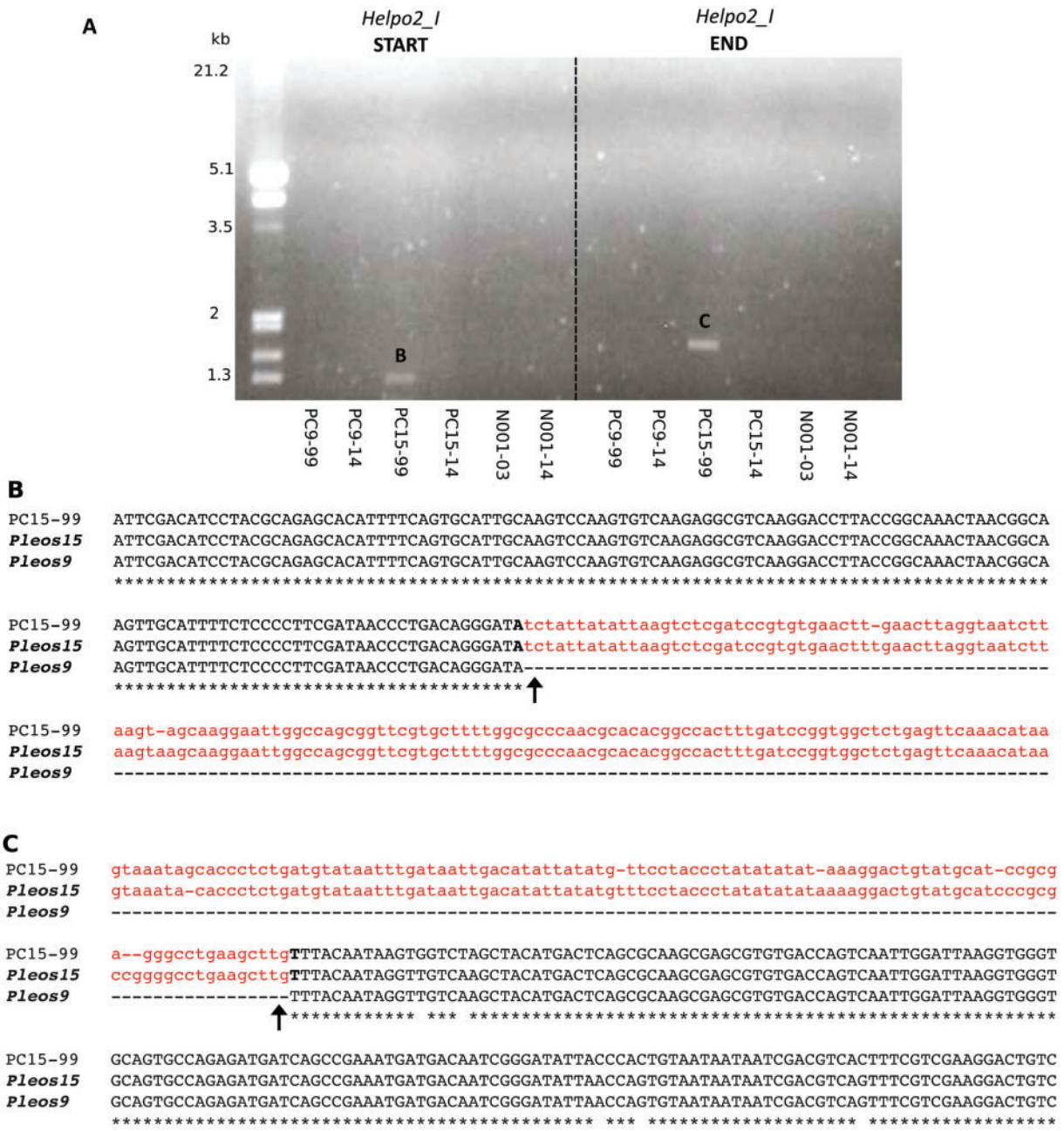

Figure 5. Evidence of HELPO2 insertion in the *Helpo2_I* locus of the PC15-99 subclone. Left (START) and right (END) *Helpo2_I* boundaries amplified exclusively in PC15-99 subclone (A). Helitron insertion in the PC15-99 subclone is reported by aligning both sequenced PCR products (B and C) to the occupied and empty sites of PC15 v2.0 (*Pleos15*) and PC9 v1.0 (*Pleos9*) reference genomes. Lowercase typeface indicates helitron sequences.

amplification products shown in Fig. 8A and B were sequenced and aligned to both PC15 v2.0 and PC9 v1.0 assemblies. SNPs were manually identified in the alignments and used to assign their parental origin. In 94% of the monokaryons analysed, the four regions studied were inherited from PC9, pointing to a preferential inheritance of the vacant site instead of a HELPO2 excision during meiosis. Nevertheless, a surprising profile was found in seven monokaryons (four in *Helpo2_VI* locus and three in *Helpo2_VIII_b* locus). Although the three flanking sites were inherited from the PC15 parental strain, SNPs of the amplification product corresponding to the vacant site (1,489 bp in *Helpo2_VI* and 907 bp in *Helpo2_VIII_b*) indicated that they were transmitted from the parental PC9 (Fig. 8A and B). These results might be explained by a mechanism of allelic gene conversion, which results in the loss of HELPO2 helitrons. To verify this hypothesis, the presence of gene conversion junctions were validated in the seven monokaryons by PCR as shown in Fig. 8C. To ensure the linearity of the short regions located between the amplified regions (shown in Fig. 8A and B as white rectangles), primers were designed to amplify longer regions, spanning *Helpo2_VI* and *Helpo2_VIII_b* loci as well as their flanking sites (Fig. 8C, Supplementary Table S6). Our results showed the presence of bands corresponding to the expected size, confirming the linearity of such

Downloaded from https://academic.oup.com/dnaresearch/article-abstract/24/2/103/2962881
by Universidad Pública de Navarra user
on 09 August 2018

Table 2. Helitrons described *in silico* in *P. ostreatus* PC15 genome assembly v2.0

Locus	Localization (chromosome[a])	Start (bp)	End (bp)	Length (bp)
Helpo2_I	I	619,761	626,150	6,388
Helpo2_V	V	387,607	398,218	10,611
Helpo2_VI	VI	1,150,050	1,156,438	6,388
Helpo2_VII	VII	1,635,256	1,641,644	6,388
Helpo2_VIII_a	VIII	1367,660	1,374,048	6,388
Helpo2_VIII_b	VIII	1,722,302	1,726,240	3,938
Helpo2_VIII_c	VIII	2,234,922	2,241,310	6,388

[a]Chromosomes are equivalent to scaffolds in PC15 v2.0 assembly.

Table 3. Molecular validation of HELPO2 polymorphisms using the PCR outer/inner strategy

	Strain					
Locus	PC9-99	PC9-14	PC15-99	PC15-14	N001–03	N001–14
Helpo2_I	Vacant	Vacant	**Occupied**	**Vacant**	Vacant	Vacant
Helpo2_V	Vacant	Vacant	Occupied	Occupied	Occupied	Occupied
Helpo2_VI	Vacant	Vacant	Occupied	Occupied	Occupied	Occupied
Helpo2_VII	Vacant	Vacant	Occupied	Occupied	Occupied	Occupied
Helpo2_VIII_a	Vacant	Vacant	Occupied	Occupied	Occupied	Occupied
Helpo2_VIII_b	Vacant	Vacant	Occupied	Occupied	Occupied	Occupied
Helpo2_VIII_c	Vacant	Vacant	**Occupied**[a]	**Vacant**	Vacant	Vacant

Each term represents an amplification product. Primers and expected product sizes are shown in Supplementary Table S2.
[a]The right flank displayed a higher size than the bioinformatics prediction (2 kb instead of 1.38 kb).

Table 4. Molecular validation of HELPO2 polymorphisms using the PCR outer/outer strategy

	Strain					
Locus	PC9-99	PC9-14	PC15-99	PC15-14	N001-03	N001-14
Helpo2_I	Vacant	Vacant	**Vacant**	Vacant	Vacant	Vacant
Helpo2_V	Vacant	Vacant				
Helpo2_VI	Vacant	Vacant				
Helpo2_VII	N/A	N/A				
Helpo2_VIII_a	Vacant	Vacant				
Helpo2_VIII_b	Vacant	Vacant				
Helpo2_VIII_c	Vacant	Vacant	**Vacant**	Vacant	Vacant	Vacant

Each term represents an amplification product. Cells in normal typeface show results in agreement with the outer/inner strategy, and in bold typeface result in disagreement. Grey cells represent occupied loci previously validated by the outer/inner strategy. Primers and expected product sizes are shown in Supplementary Table S3.
N/A, no amplification.

regions and discarding the presence of rearrangements (Supplementary Fig. S4). After sequencing, PCR products were aligned to both PC15 and PC9 parental strains. Interestingly, the pattern of SNPs/indels showed that gene conversion occurred precisely in the same sites in all monokaryons analysed for each locus (Supplementary Fig. S5), suggesting that the mechanism leading to this recombination might have specific targets. The absence of HELPO2 helitrons in the monokaryons with profiles consistent with allelic gene conversion events suggests that this mechanism might be used to eliminate unpaired repetitive sequences (such TEs) during meiosis. Allelic gene conversion is a molecular mechanism associated with recombination in which a genomic fragment is 'copied/pasted' onto another homologous fragment. Little is known about gene conversion in fungi, although it is associated with non-Mendelian segregation ratios in yeast and mammals.[43,44] In fungi, previous studies have shown that gene conversion leads to 3:1 ratios in heteroallelic crosses.[45] A recent analysis of the recombination landscape in the basidiomycete *Agaricus bisporus* revealed a skewed segregation ratio from the expected Mendelian 1:1 in certain loci of the haploid offspring of 139 isolated single spores. In addition, results showed that crossover events (COs) occurred almost exclusively at chromosome ends including gene conversion in the reciprocal CO context.[46] In 1982, it was proposed that gene conversion could be involved in the elimination of selfish DNA during meiosis when hybrid DNA structures are homologous but one of them displays a DNA insert present in one parent,[47] as is

Downloaded from https://academic.oup.com/dnaresearch/article-abstract/24/2/103/2962881
by Universidad Pública de Navarra user
on 09 August 2018

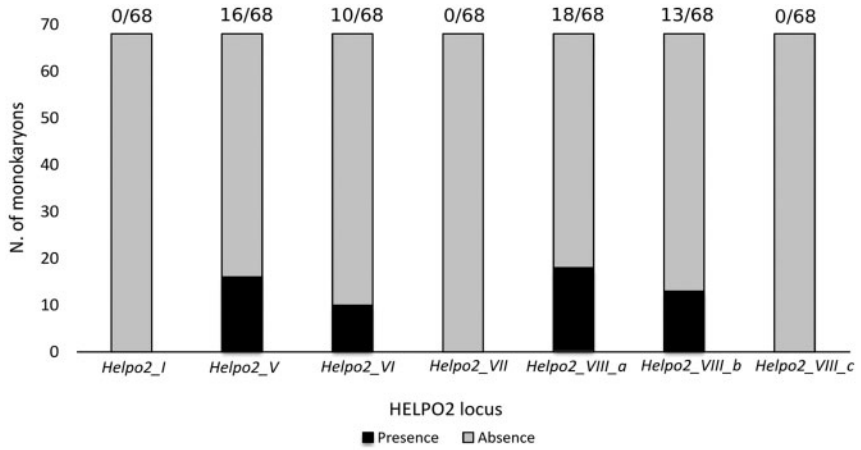

Figure 6. HELPO2 segregation rates in the 68-mK monokaryotic progeny. Distribution of HELPO2 helitrons in a meiotic progeny of 68 individuals is reported as stacked histograms. The seven HELPO2 loci are shown on the X-axis. The Y-axis indicates the number of monokaryons. Black and grey bars show the number of monokaryons presenting occupied and vacant loci, respectively. The frequency of helitron presence per locus is shown above each bar.

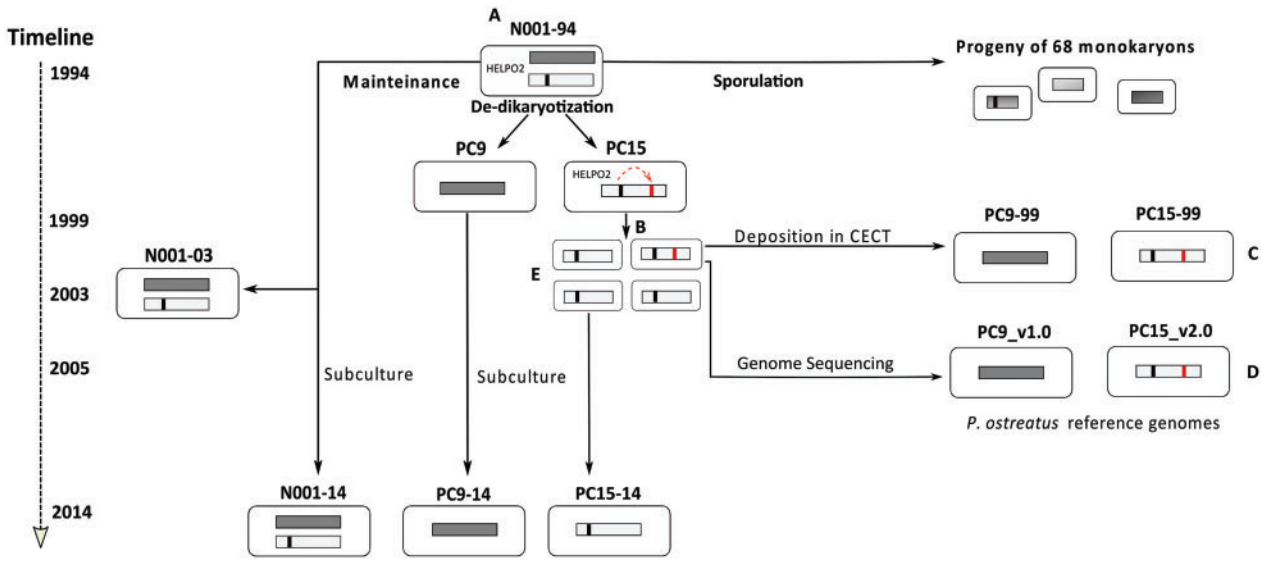

Figure 7. Chronological model explaining HELPO2 somatic insertions in the PC15-99 subclone. (a) (1994) N001-94 parental strain displays 4 helitron loci (*Helpo2_V, Helpo2_VI, Helpo2_VIII_a* and *Helpo2_VIII_b*), which are transmitted to the meiotic progeny 68 mK. (b) (1999). After de-dikaryotization, a HELPO2 from one of the four loci mobilizes in a cell of PC15 and integrates into a new locus (i.e. *Helpo2_I*), producing a mosaic mycelium displaying both occupied (*Helpo2_I+)* and vacant (*Helpo2_I)* cells (dashed arrow indicates HELPO2 helitron transposition and subsequent integration). (c) (1999–2014) A PC15 subclone presenting mosaicism is deposited in the CECT and maintained under low subculture frequency up to 2014 (PC15-99). (d) (2005) A PC15 subclone carrying *Helpo2_I+* cells is used for whole genome sequencing by JGI. (e) (1999–2014) PC15 subclone used for routine laboratory work up to 2014 (PC15-14) is derived from a section of PC15 *Helpo2_I-* cells. Alternatively, *Helpo2_I+* cells were lost by random drift as a consequence of the high subculture frequency.

the case with HELPO2 loci in PC15 and PC9. In such a case, a single-strand loop could be formed, being targeted by endonucleases and resulting in gene conversion with the elimination of the insert. Events of a model of gene conversion mediated by site-specific endonucleases have also been detected in different strains of *Botrytis cinerea*. The analysis of meiotic products obtained by crossing strains carrying polymorphisms permitted determination of gene conversion tracts that corresponded to unpaired regions previously identified in the parental strains.[48] Our results are the first showing evidence of the somatic transposition of a native helitron in its own host and the meiotically driven elimination of an active helitron family in basidiomycetes.

3.7. Helitron elimination in *P. ostreatus* progeny: genome defence against invasive DNA?

Eukaryotes have developed defence mechanisms to control the proliferation of TEs and avoid the potentially harmful effects of their insertions. One of the most impressive mechanisms of genome defence is called chromatin diminution, which has been described in several eukaryotes from distinct lineages.[49,50] This mechanism selectively eliminates DNA and targets mainly young TEs displaying high frequencies and similarities.[49] The molecular mechanism underlying chromatin diminution bears similarity to piRNA-directed transposon silencing in metazoans and requires an active RNAi machinery. In fact, it has been proposed that small RNAs could play an essential role directing such

Downloaded from https://academic.oup.com/dnaresearch/article-abstract/24/2/103/2962881
by Universidad Pública de Navarra user
on 09 August 2018

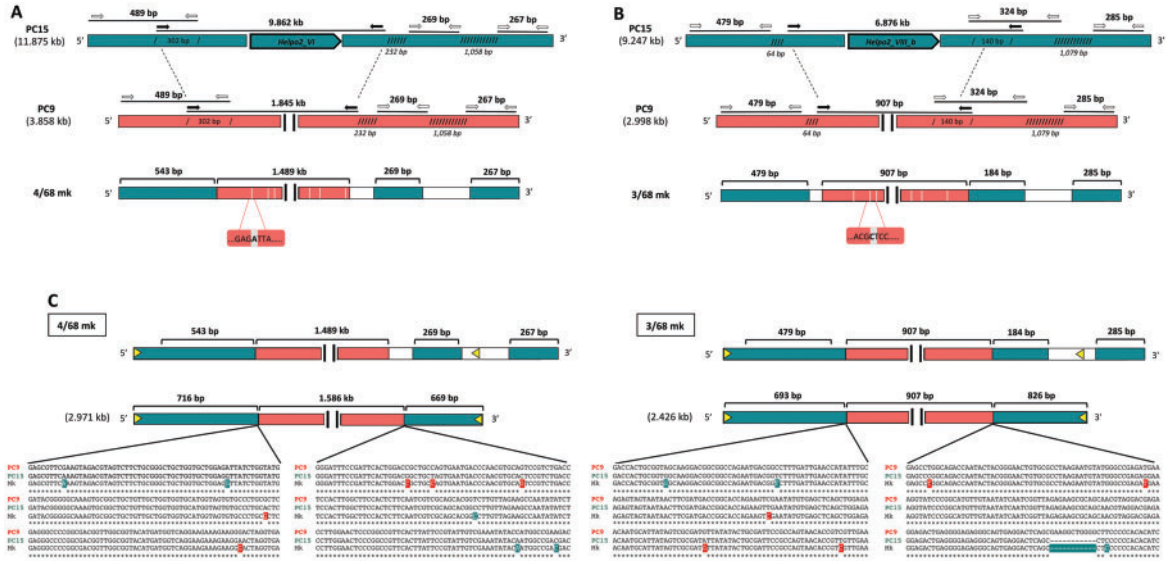

Figure 8. Molecular validation of HELPO2 meiotic loss. Schematic representation of *Helpo2_VI* (A), *Helpo2_VIII_b* (B) loci and their flanking (homologous) regions in the parental PC15 (upper blocks) and PC9 (intermediate blocks) as well as in 7 monokaryons showing profiles compatible with gene conversion events (lower blocks). HELPO2 elements are represented as an arrow in the parental PC15, but are absent in PC9 (vertical black lines). PCR primers are represented by black arrows (designed to amplify the vacant site) and white arrows (designed to amplify flanking sites). The size of overlapping regions (bp) amplified by primers pairs is showed between two slashes in PC15 and PC9 sequences. Regions excluded to PCR amplification are indicated by slashes in PC15 and PC9 parental strains and white rectangles in monokaryons. Vertical grey lines inside blocks represent PC9-specific SNPs/indels used to assign the parental origin of such regions. (C) Validation of gene conversion event in 4 (*Helpo2_VI* locus) and 3 (*Helpo2_VIII_b* locus) monokaryons. Primers sequences are indicated by arrows. Gene conversion junctions with their associated SNPs/indels are reported in the DNA alignment.

Table 5. Identification of proteins belonging to the RNAi pathway in *P. ostreatus*

PC15-ID[a]	PC9-ID[a]	RPKM	RPKM	Description
25449	90477	10.8	11.1	RNA-dependent RNA polymerase
1053861	85609	16.34	30.2	RNA-dependent RNA polymerase
1076136	83385	2.74	0.6	RNA-dependent RNA polymerase
1041769	52011	36.06	22.6	RNA-dependent RNA polymerase
154946	85193	53.19	21.8	RNA-dependent RNA polymerase
1060211	89407	87.2	233.8	Argonaute
1110274	43687	116.78	59.7	Argonaute
173501	122655	85.31	124.2	Argonaute
21640	91748	12.43	20.5	Argonaute
44554	114784	27.76	39.9	Argonaute
33722	67302	15.34	30.7	RecQ Helicase
11210	24796	12.58	3.3	RecQ Helicase
160303	87316	7.47	4.8	RecQ Helicase
1064031	83509	12.96	6.6	DICER
1033048	81629	9.4	7.6	DICER
1093523	50672	27.64	16.8	DICER
1112895	84917	34.41	47.1	DICER
1039826	83395	41.63	54.4	DnaQ-like exonuclease

Transcription of PC15 and PC9 orthologs is shown in RPKM (reads per kilobase per million mapped reads).

[a]Protein identifiers of PC15 v2.0 and PC9 v1.0 Mycocosm databases.

DNA elimination in the protozoan *Tetrahymena thermophile*.[50] No study has described the presence of such mechanisms in fungi, but a handful of studies have shown the presence and activity of the main components of the RNAi pathway in filamentous fungi (Dicer, Argonaute, and RNA-dependent RNA polymerase, reviewed in Ref. 51). From the diversity of the fungal RNAi pathway, two mechanisms have evolved to control TEs at the vegetative (Quelling) and sexual (MSUD) states. The latter is of great relevance to our study as it involves the identification of unpaired DNA during meiosis by a *trans*-sensing mechanism. The origin of such unpaired regions are likely produced by TE insertions in only one of the two parental strains, such as in the case of the HELPO2 family in *P. ostreatus*. We screened PC15 and PC9 genomes for proteins homologous to those involved in *N. crassa* MSUD and Quelling and found a total of 18 genes in both strains: 5 argonaute proteins, 5 RNA-dependent RNA polymerases (RdRPs), 4 dicers, 3 RecQ helicases and 1 exonuclease. *P. ostreatus* RNAi proteins carry the corresponding conserved domains (Supplementary Table S7) and are actively expressed in vegetative mycelia (Table 5). Further experimental work is needed to understand whether the transcriptional repression and meiotic elimination of HELPO2 is somehow linked to the activity of RNAi pathway genes. Due to the ability of fungi to diversify and develop 'epigenetic solutions' to control TE proliferation, such a possibility seems to be an interesting field for future studies.

Acknowledgements

We would like to thank Dr. Matteo Pellegrini and Marco Morselli (University of California, Los Angeles) for the lab equipment support.

Conflict of interest

None declared.

Footnotes

Conceived and designed the experiments: AB RC AGP LR. Performed the experiments: AB EM. Analyzed the data: AB RC LR. Wrote the paper: AB

Downloaded from https://academic.oup.com/dnaresearch/article-abstract/24/2/103/2962881
by Universidad Pública de Navarra user
on 09 August 2018

RC. Led the project, revised and edited the manuscript: AGP LR. All been deposited in databases.

Supplementary data

Supplementary data are available at www.dnaresearch.oxfordjournals.org.

Funding

This work was supported by Spanish National Research Plan (Projects AGL2011-30495 and AGL2014-55971-R) and FEDER funds; Public University of Navarre (http://www.unavarra.es); AB holds a PhD scholarship from the Public University of Navarre and RC holds a FPI-PhD scholarship from the Ministry of Economy and Competitiveness.

References

1. Kazazian, H. H. 2004, Mobile elements: drivers of genome evolution. *Science*, **303**, 1626–32.
2. Wicker, T., Sabot, F., Hua-Van, A., et al. 2007, A unified classification system for eukaryotic transposable elements. *Nat. Rev. Genet.*, **8**, 973–82.
3. Kapitonov, V. V, and Jurka, J. 2001, Rolling-circle transposons in eukaryotes. *Proc. Natl. Acad. Sci. U. S. A.*, **98**, 8714–9.
4. Poulter, R. T. M., Goodwin, T. J. D., and Butler, M. I. 2003, Vertebrate helentrons and other novel Helitrons. *Gene*, **313**, 201–12.
5. Pritham, E. J., and Feschotte, C. 2007, Massive amplification of rolling-circle transposons in the lineage of the bat *Myotis lucifugus*. *Proc. Natl. Acad. Sci. U. S. A.*, **104**, 1895–900.
6. Roffler, S., Menardo, F., and Wicker, T. 2015, The making of a genomic parasite - the Mothra family sheds light on the evolution of Helitrons in plants. *Mob. DNA*, **6**, 23.
7. Kapitonov, V. V., and Jurka, J. 2007, Helitrons on a roll: eukaryotic rolling-circle transposons. *Trends Genet.*, pp. 521–9.
8. Li, Y., and Dooner, H. K. 2009, Excision of Helitron transposons in maize. *Genetics*, **182**, 399–402.
9. Lai, J., Li, Y., Messing, J., and Dooner, H. K. 2005, Gene movement by Helitron transposons contributes to the haplotype variability of maize. *Proc. Natl. Acad. Sci. U. S. A.*, **102**, 9068–73.
10. Choi, J. D., Hoshino, A., Park, K. Il, Park, I. S., and Iida, S. 2007, Spontaneous mutations caused by a Helitron transposon, Hel-It1, in morning glory, *Ipomoea tricolor*. *Plant J.*, **49**, 924–34.
11. Fu, H., and Dooner, H. K. 2002, Intraspecific violation of genetic colinearity and its implications in maize. *Proc. Natl. Acad. Sci. U. S. A.*, **99**, 9573–8.
12. Grabundzija, I., Messing, S. A., Thomas, J., et al. 2016, A Helitron transposon reconstructed from bats reveals a novel mechanism of genome shuffling in eukaryotes. *Nat. Commun.*, **7**, 10716.
13. Zhou, Q., Froschauer, A., Schultheis, C., et al. 2006, Helitron Transposons on the Sex Chromosomes of the Platyfish *Xiphophorus maculatus* and Their Evolution in Animal Genomes. *Zebrafish*, **3**, 39–52.
14. Lal, S. K. 2003, The Maize Genome Contains a Helitron Insertion. *Plant Cell Online*, **15**, 381–91.
15. Xiong, W., He, L., Lai, J., Dooner, H. K., and Du, C. 2014, HelitronScanner uncovers a large overlooked cache of Helitron transposons in many plant genomes. *Proc. Natl. Acad. Sci.*, **111**, 10263–8.
16. Morgante, M., Brunner, S., Pea, G., Fengler, K., Zuccolo, A., and Rafalski, A. 2005, Gene duplication and exon shuffling by helitron-like transposons generate intraspecies diversity in maize. *Nat. Genet.*, **37**, 997–1002.
17. Castanera, R., Perez, G., Lopez, L., et al. 2014, Highly expressed captured genes and cross-kingdom domains present in Helitrons create novel diversity in *Pleurotus ostreatus* and other fungi. *BMC Genomics*, **15**, 1071.
18. Cultrone, A., Domínguez, Y. R., Drevet, C., Scazzocchio, C., and Fernández-Martín, R. 2007, The tightly regulated promoter of the xanA gene of *Aspergillus nidulans* is included in a helitron. *Mol. Microbiol.*, **63**, 1577–87.
19. Martin, F., Kohler, A., Murat, C., et al. 2010, Périgord black truffle genome uncovers evolutionary origins and mechanisms of symbiosis. *Nature*, **464**, 1033–8.
20. Labbé, J., Murat, C., Morin, E., Tuskan, G. A., Le Tacon, F., and Martin, F. 2012, Characterization of transposable elements in the ectomycorrhizal fungus *Laccaria bicolor*. *PLoS One*, **7**.
21. Santoyo, F., González, A. E., Terrón, M. C., Ramírez, L., and Pisabarro, A. G. 2008, Quantitative linkage mapping of lignin-degrading enzymatic activities in *Pleurotus ostreatus*. *Enzyme Microb. Technol.*, **43**, 137–43.
22. Eugenio, C. P., and Anderson, N. A. 1968, The genetics and cultivation of *Pleurotus ostreatus*. *Mycologia*, **60**, 627.
23. Sánchez, C. 2010, Cultivation of *Pleurotus ostreatus* and other edible mushrooms. *Appl. Microbiol. Biotechnol.*, **85**, 1321–37.
24. Larraya, L. M., Perez, G., Peñas, M. M., et al. 1999, Molecular karyotype of the white rot fungus *Pleurotus ostreatus*. *Appl. Envir. Microbiol.*, **65**, 3413–7.
25. Larraya, L. M., Perez, G., Ritter, E., Pisabarro, A. G., and Ramírez, L. 2000, Genetic linkage map of the edible basidiomycete *Pleurotus ostreatus*. *Appl. Environ. Microbiol.*, **66**, 5290–300.
26. Park, S.-K., Peñas, M. M., Ramírez, L., and Pisabarro, A. G. 2006, Genetic linkage map and expression analysis of genes expressed in the lamellae of the edible basidiomycete *Pleurotus ostreatus*. *Fungal Genet. Biol. FG B*, **43**, 376–87.
27. Castanera, R., López-Varas, L., Borgognone, A., et al. 2016, Transposable elements versus the fungal genome: impact on whole-genome architecture and transcriptional profiles. *PLoS Genet.*, **12**, e1006108.
28. Larraya, L. M., Alfonso, M., Pisabarro, A. G., and Ramírez, L. 2003, Mapping of genomic regions (quantitative trait loci) controlling production and quality in industrial cultures of the edible basidiomycete *Pleurotus ostreatus*. *Appl. Environ. Microbiol.*, **69**, 3617–25.
29. Riley, R., Salamov, A. A., Brown, D. W., et al. 2014, Extensive sampling of basidiomycete genomes demonstrates inadequacy of the white-rot/brown-rot paradigm for wood decay fungi. *Proc. Natl. Acad. Sci. U. S. A.*, **111**, 9923–8.
30. Alfaro, M., Castanera, R., Lavín, J. L., et al. 2016, Comparative and transcriptional analysis of the predicted secretome in the lignocellulose-degrading basidiomycete fungus *Pleurotus ostreatus*. *Environ. Microbiol.*
31. Untergasser, A., Cutcutache, I., Koressaar, T., et al. 2012, Primer3-new capabilities and interfaces. *Nucleic Acids Res.*, **40**.
32. Altschul, S. F., Gish, W., Miller, W., Myers, E. W., and Lipman, D. J. 1990, Basic local alignment search tool. *J. Mol. Biol.*, **215**, 403–10.
33. Pfaffl, M. W. 2001, A new mathematical model for relative quantification in real-time RT-PCR. *Nucleic Acids Res.*, **29**, e45.
34. Eddy, S. R. 2011, Accelerated Profile HMM Searches Pearson, W. R., (ed.), . *PLoS Comput. Biol.*, **7**, e1002195.
35. Finn, R. D., Bateman, A., Clements, J., et al. 2014, Pfam: the protein families database. *Nucleic Acids Res.*, **42**, D222–30.
36. Marchler-Bauer, A. et al. 2015, CDD: NCBI's conserved domain database. *Nucleic Acids Res.* **43**, D222–D226.
37. Enright, A. J., Dongen, S. Van, and Ouzounis, C. A. 2002, An efficient algorithm for large-scale detection of protein families. *Nucleic Acids Res.*, **30**, 1575–84.
38. Naas, T., Blot, M., Fitch, W. M., and Arber, W. 1994, Insertion Sequence-Related Genetic-Variation In Resting *Escherichia Coli* K-12. *Genetics*, **136**, 721–30.
39. Capy, P., Gasperi, G., Biémont, C., and Bazin, C. 2000, Stress and transposable elements: co-evolution or useful parasites?. *Heredity (Edinb).*, **85**, 101–6.
40. Tittel-Elmer, M., Bucher, E., Broger, L., Mathieu, O., Paszkowski, J., and Vaillant, I. 2010, Stress-induced activation of heterochromatic transcription. *PLoS Genet.*, **6**, 1–11.
41. Peabody, R. B., Peabody, D. C., and Sicard, K. M. 2000, A genetic mosaic in the fruiting stage of *Armillaria gallica*. *Fungal Genet. Biol.*, **29**, 72–80.

Downloaded from https://academic.oup.com/dnaresearch/article-abstract/24/2/103/2962881
by Universidad Pública de Navarra user
on 09 August 2018

42. Peabody, R. B., Peabody, D. C., Tyrrell, M. G., Edenburn-MacQueen, E., Howdy, R. P., and Semelrath, K. M. 2005, Haploid vegetative mycelia of *Armillaria gallica* show among-cell-line variation for growth and phenotypic plasticity. *Mycologia*, **97**, 777–87.
43. Lamb, B. C. 1998, Gene conversion disparity in yeast: its extent, multiple origins, and effects on allele frequencies. *Heredity (Edinb)*, **80** (Pt 5), 538–52.
44. Galtier, N. 2001, GC-Content Evolution in Mammalian Genomes: The Biased Gene Conversion Hypothesis. *Dev. Psychobiol.*, **39**, 251–6.
45. Holliday, R. 2007, A mechanism for gene conversion in fungi. *Genet. Res.*, **89**, 285–307.
46. Sonnenberg, A. S. M., Gao, W., Lavrijssen, B., et al. 2016, A detailed analysis of the recombination landscape of the button mushroom *Agaricus bisporus var. bisporus*. *Fungal Genet. Biol.*, **93**, 35–45.
47. Holliday, R. 1982, Gene Conversion: A Possible Mechanism for Eliminating Selfish DNA. *Molecular and Cellular Mechanisms of Mutagenesis*. Springer US, Boston, MA, pp. 259–64.
48. Bokor, A. A. M., van Kan, J. A. L., and Poulter, R. T. M. 2010, Sexual mating of *Botrytis cinerea* illustrates PRP8 intein HEG activity. *Fungal Genet. Biol.*, **47**, 392–8.
49. Sun, C., Wyngaard, G., Walton, D., et al. 2014, Billions of basepairs of recently expanded, repetitive sequences are eliminated from the somatic genome during copepod development. *BMC Genomics*, **15**, 186.
50. Kataoka, K., and Mochizuki, K. 2011, Programmed DNA elimination in tetrahymena: A small RNA-mediated genome surveillance mechanism. *Adv. Exp. Med. Biol.*, **722**, 156–73.
51. Dang, Y., Yang, Q., Xue, Z., and Liu, Y. 2011, RNA interference in fungi: Pathways, functions, and applications. *Eukaryot. Cell*, pp. 1148–55.

Downloaded from https://academic.oup.com/dnaresearch/article-abstract/24/2/103/2962881
by Universidad Pública de Navarra user
on 09 August 2018